

Chapter 5

Interference-Constrained Power-Adaptive Decode-and-Forward Relaying Policy

This chapter presents an interesting application of cooperative communication techniques in cognitive radio systems or spectrum sharing systems (SSS). For the analysis, we have considered two system models, that are, i.) non-energy harvesting (N-EH) relay-assisted cooperative SSS (C-SSS) system model, and ii.) energy harvesting (EH) relay-assisted C-SSS system model. We propose an interference-constrained power-adaptive decode-and-forward (IC-PA-DAF) relaying policy that optimally enhances the performance measures for each system model. Apart from DAF operations, the proposed relaying policy optimally sets its relay gain based on the channel characteristics of its local links. For both the system models, we optimize the FASE and FAEE performance measures. The organization of this chapter is as follows.

We initially consider an N-EH relay-assisted C-SSS. In Section 5.1, we describe the system model and its assumptions. Section 5.2 illustrates the optimization problem to derive optimum RGF for both FASE and FAEE and then present the optimal expression for FASE and FAEE and its upper bounds. Further, in Section 5.3, we present the numerical results based on the derived analytical expressions and compare them with the benchmark policies. To increase the complexity of the system model, we present EH relay-assisted C-SSS in Section 5.4. For the EH system model, the optimization problem and the performance analysis are shown in Section 5.5. Furthermore, numerical results and benchmark comparison are presented in Section 5.6. Lastly, the summary of the work presented in this chapter is shown in Section 5.7.

5.1 Non-EH Relay-Assisted C-SSS Model

Figure 5.1 illustrates a secondary cloud having four secondary user (SU) nodes in an underlay C-SSS. In it, the SU source node S_{Tx}^S transmits the signal to the SU destination node D_{Rx}^S with either of the cooperative IC-PA-DAF relay nodes R_1^S / R_2^S . Relay nodes are essential since the D_{Rx}^S node is not in the transmission range of the S_{Tx}^S node [97]. Nodes outside the secondary cloud are primary user (PU) [139]. The PU

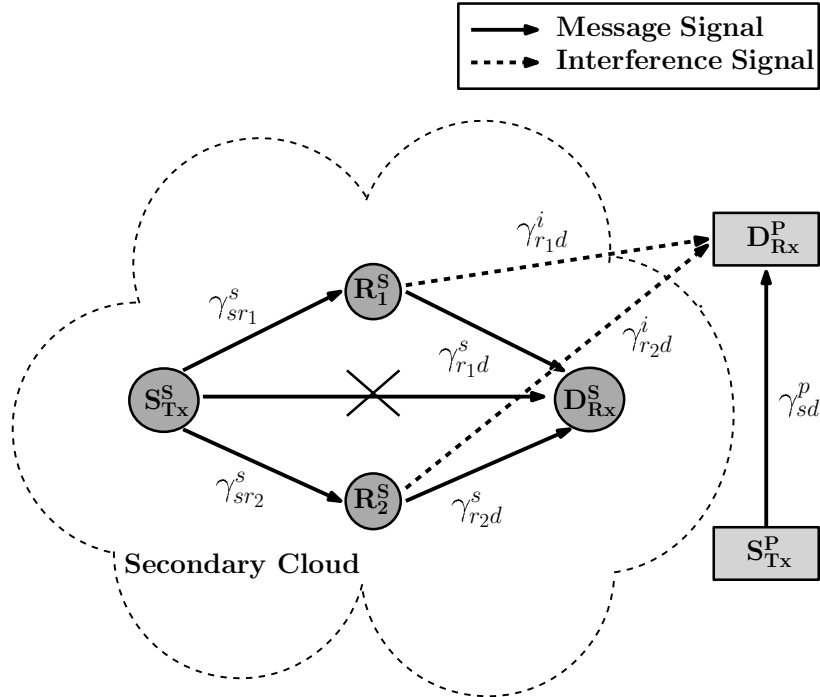


Figure 5.1: IC-PA-DAF relay-assisted underlay C-SSS model.

source node S_{Tx}^P is also transmitting the signal to the PU destination node D_{Rx}^P [139]. Note that the underlay mode of C-SSS is adopted in the system model [140]. Therefore, the secondary relay nodes need to transmit their signal such that it should not cause average interference at the D_{Rx}^P node above a certain threshold [141]. Furthermore, we assume that the interference caused by S_{Tx}^S at D_{Rx}^P is negligible as the nodes are sufficiently far away [36].

In the proposed power-adaptive underlay C-SSS model, we assume that all the nodes have a single transmitting and receiving antenna [98]. Further, all the nodes transmitting the signal in the system model stick to the same transmission frequency [98]. We assume that the complex fading channel gains between all the nodes are statistically independent of each other and follow frequency-flat block fading distribution [99]. Furthermore, we also assume AWGN components due to system electronics and are statistically independent of all fading channel gains [35]. Though we consider single antenna nodes, it is possible to make more complex fading models and nodes with multiple antennas.

Remarks on the interference by the PU transmitter on the SU nodes: Note that the interference does exist at the secondary underlay node due to the transmissions from the PU source. However, by assuming Gaussian interference [36], the interference can be implicitly accounted for in the noise variance term. The Gaussian interference assumption is valid because of the central limit theorem where several primary nodes are present. Specifically, let σ_w^2 , and σ_i^2 denote the noise variance and interference

variance, respectively. Therefore, the total variance of the undesired components (noise and variance) $\sigma_n^2 = \sigma_w^2 + \sigma_i^2$.

Alternatively, secondary destination nodes could employ interference mitigation techniques for scenarios where the Gaussian assumption is invalid. However, these signal processing techniques for interference mitigation or cancellation add additional complexity to nodes in the C-SSS.

- *Implementation of successive interference cancellation (SIC)*: Implementing SIC at the secondary destination can overcome the effect of interference from other users [142]. SIC recovers the desired secondary relay transmitted signal at the secondary destination by subtracting the decoded interference signal.
- *Pattern reconfigurable antennas*: Radiation pattern reconfigurable antennas or directional antennas adjust the radiation pattern while the transmitted signal frequency remains unchanged [141]. These antennas can steer the radiating signal to a particular direction to increase the signal quality at the intended receiver and reduce interference at the unintended receivers, that is, the secondary destination receivers in the proposed C-SSS model.

5.1.1 Comparison of Different SSS modes

In the thesis, we proposed efficient policies for underlay cooperative spectrum sharing systems. We considered the underlay mode due to its advantages in terms of superior spectral efficiency. However, the transmission of the secondary IC-PA-DAF relay node can take place in two other modes also: interweave and overlay mode. Below we discuss the impact of the modes on the proposed system model.

- *Secondary node in interweave mode*: In this mode, the secondary relay transmits opportunistically when the primary source is not accessing the channel [141]. In this mode, the simultaneous transmission of the secondary regenerative relay and the primary source is prohibited. Therefore, the secondary user's transmit power is constrained by the spectral hole sensing range [143]. Furthermore, the performance of the interweave-mode system depends on the spectral hole detection probability.
- *Secondary node in overlay Mode*: In comparison to the interweave mode, both the secondary relay and the primary source can access the channel concurrently in overlay mode [141]. For the concurrent transmission, secondary nodes need to know about the channel state information (CSI), codebooks, and message

signal of the primary nodes. Furthermore, the transmit power of the secondary regenerative relay is not constrained in this mode [143].

The detailed analysis of the interweave-mode or overlay-mode SSS is beyond the scope of the thesis and is a potential future work. However, the former system's optimal performance depends on the probability of successfully detecting spectrum holes, which requires a highly accurate energy detector. On the other hand, the performance of the overlay depends on the accurate information available with the secondary nodes, which is not always possible, especially in delay-sensitive applications.

Based on the fundamental features of modes of spectrum sharing systems, we see that overlay and underlay mode are more spectrally efficient since concurrent transmission is possible [141, 144]. Furthermore, overlay mode requires a large amount of side information and complex encoding and decoding to avoid interference in comparison to underlay mode [141]. Since the underlay mode spectrum sharing system is more spectrally efficient and relatively easier to implement, we assumed underlay mode for the analysis in this thesis.

5.1.2 Non-EH Relay-Assisted C-SSS Transmission Protocol

Information transmission from S_{Tx}^S to D_{Rx}^S takes place in two-phases, that is the broadcasting phase and the forwarding phase. In the broadcasting phase, S_{Tx}^S broadcast the information signal x to the relay nodes, that is, R_1^S and R_2^S in the secondary cloud. We assume that the information symbol x has unit energy. Furthermore, it is also assumed that the transmit power of secondary source node is set such that the relay nodes are able to decode the signal correctly.

In the forwarding phase, the selected IC-PA-DAF relay node (R_1^S or R_2^S) on receiving the information signal from S_{Tx}^S , first perform decoding. Later, the relay performs re-encoding, and then adaptively amplifies the signal to be forwarded based on relay gain function (RGF). The RGF is dependent on the channel power gain of the relay to the PU's receiver link and relay to the SU's receiver link. Therefore, RGF ($\psi(\gamma_{r_1d}^s, \gamma_{r_2d}^s, \gamma_{r_1d}^i, \gamma_{r_2d}^i)$) is the function of channel power gain of $R_1^S - D_{Rx}^S$ link ($\gamma_{r_1d}^s$), $R_2^S - D_{Rx}^S$ link ($\gamma_{r_2d}^s$), $R_1^S - D_{Rx}^P$ link ($\gamma_{r_1d}^i$), and $R_2^S - D_{Rx}^P$ link ($\gamma_{r_2d}^i$). Further, the IC-PA-DAF relay (selected as the best relay based on the PRSP) re-transmits the amplified signal to the D_{Rx}^S while satisfying the average interference constraint.

Remarks: The transmit-power control at the secondary relay is a non-trivial problem, specifically at dynamic channel conditions. However, in the system model considered in this thesis, all the nodes are static, and the end-to-end data transmission takes place in two timeslots. We assume that the frequency-flat Rayleigh fading chan-

nel remains quasi-static over the two-time slots. Furthermore, transmit power control at the secondary user in dynamic channel conditions caused by the mobility of nodes (for example, vehicular communication channels) can be a potential future work.

5.1.3 Remarks on Relay Selection

As discussed earlier, relay selection helps improve bandwidth efficiency and reduce hardware complexity and synchronization problem. Therefore in this chapter, we use PRSP for selecting the IC-PA-DAF relay. Note that the PRSP is a partial relay selection policy, which requires statistical CSI of a secondary source to the secondary relay link only. In the PRSP, IC-PA-DAF relay R_1^S is selected if the probability of instantaneous SNR of $S_{Tx}^S - R_1^S$ link is greater than the instantaneous SNR of $S_{Tx}^S - R_2^S$ link, that is, $p_1 \triangleq \mathcal{P}(\Gamma_{r_1} > \Gamma_{r_2})$. If the previous condition is not satisfied, the IC-PA-DAF relay R_2^S is selected, and this condition is mathematically written as $p_2 \triangleq \mathcal{P}(\Gamma_{r_1} < \Gamma_{r_2})$. Note that both Γ_{r_1} and Γ_{r_2} are exponentially distributed; therefore, p_1 and p_2 can be expressed as $\frac{\alpha}{\alpha+\beta}$ and $\frac{\beta}{\alpha+\beta}$, respectively (for proof refer to Appendix A.1 of the thesis). Where α and β are average SNR of $S_{Tx}^S - R_1^S$ link and $S_{Tx}^S - R_2^S$ link, respectively. Mathematically, $\alpha = \frac{P_s \bar{\gamma}_{sr_1}^s}{\sigma_n^2}$ and $\beta = \frac{P_s \bar{\gamma}_{sr_2}^s}{\sigma_n^2}$, where P_s is secondary source transmit power, $\bar{\gamma}_{sr_1}^s$ and $\bar{\gamma}_{sr_2}^s$ are mean channel power gain of $S_{Tx}^S - R_1^S$ link and $S_{Tx}^S - R_2^S$ link and σ_n^2 is noise variance.

5.1.4 Remarks on CSI

To conserve space, we will represent $\psi(\gamma_{r_1d}^s, \gamma_{r_2d}^s, \gamma_{r_1d}^i, \gamma_{r_2d}^i)$ as ψ in the rest of the chapter. SU's source node S_{Tx}^S requires average CSI of $S_{Tx}^S - R_1^S$ link and $S_{Tx}^S - R_2^S$ link for IC-PA-DAF relay selection using PRSP. SU's relay nodes (R_1^S and R_2^S) require instantaneous CSI of $S_{Tx}^S - R_1^S$ link and $S_{Tx}^S - R_2^S$ link for ML detection. Further, since IC-PA-DAF relays are power-adaptive and the amplification is based on ψ , IC-PA-DAF relay has to acquire instantaneous CSI of $R_1^S - D_{Rx}^S$ link, $R_2^S - D_{Rx}^S$ link, $R_1^S - D_{Rx}^P$ link, and $R_2^S - D_{Rx}^P$ link. Furthermore, secondary destination node D_{Rx}^S also require CSI of selected IC-PA-DAF secondary relay to secondary destination link for signal decoding. Note that for PU's communication, D_{Rx}^P requires CSI of $D_{Rx}^P - S_{Tx}^P$ link for primary signal decoding. Known pilot sequences-based estimation protocols are useful in acquiring the required CSI.

5.2 Optimization and Analysis for N-EH Relay-Assisted C-SSS

This section derives expressions for two significant PHY layer performance measures, namely, FASE and FAEE. We proceed as follows. First, we formulate optimization problems for both the performance measures individually. We then derive the optimal solution, that is, the optimum RGF. Later, we evaluate optimal FASE and optimal FAEE. Note that the optimum RGF that optimizes FASE need not optimize FAEE and vice versa. Before proceeding with mathematical derivations, we first define the instantaneous SNR at the secondary destination D_{Rx}^{S} . The instantaneous SNR of the $R_1^{\text{S}} - D_{\text{Rx}}^{\text{S}}$ link, and $R_2^{\text{S}} - D_{\text{Rx}}^{\text{S}}$ link, respectively, are

$$\Gamma_{D_1} = \frac{\psi P_r \gamma_{r_1 d}^s}{\sigma_d^2 d^\nu}, \quad \text{and} \quad \Gamma_{D_2} = \frac{\psi P_r \gamma_{r_2 d}^s}{\sigma_d^2 d^\nu}, \quad (5.2.1)$$

where P_r is the relay transmit power, σ_d^2 is the noise variance, d is the distance between the SU relay to the secondary destination, and ν is path loss exponent. Note that the optimum RGF is denoted by ψ^* . In the following subsection, we analyze the optimal FASE for the system model considered.

Remarks: In this chapter, we derive optimum RGF independently for FASE and FAEE. As the objective functions in the two optimization problems are different, the optimal solutions are different. Therefore, for clarity, we represent $\psi_{\mathcal{S}}$ as RGF for FASE and $\psi_{\mathcal{E}}$ as RGF for FAEE.

5.2.1 Optimal FASE of IC-PA-DAF

In this subsection, we derive the expression for optimal FASE and its upper bound. FASE is an important PHY measure useful to evaluate the proposed policy performance. To derive the optimal FASE expression, we first state the optimization problem and obtain its solution. In the problem, FASE is the objective function, and the constraint is the average interference constraint. Mathematically, we formulate the optimization problem as

$$\max_{\psi_{\mathcal{S}}} \mathbf{E} \left[p_1 \log_2 \left(1 + \frac{\psi_{\mathcal{S}} P_r \gamma_{r_1 d}^s}{\sigma_d^2 d^\nu} \right) + p_2 \log_2 \left(1 + \frac{\psi_{\mathcal{S}} P_r \gamma_{r_2 d}^s}{\sigma_d^2 d^\nu} \right) \right], \quad (5.2.2)$$

$$\text{s.t. } \mathbf{E} \left[p_1 \frac{\psi_{\mathcal{S}} P_r \gamma_{r_1 d}^i}{\sigma_D^2 D^\nu} + p_2 \frac{\psi_{\mathcal{S}} P_r \gamma_{r_2 d}^i}{\sigma_D^2 D^\nu} \right] \leq I_{\text{th}}, \quad (5.2.3)$$

where $\mathbf{E}[\cdot]$ is the expectation, p_1 and p_2 are relay selection probabilities, σ_D^2 is the noise variance of the relay to primary destination, D is the distance of $R_1^S - D_{R_x}^P$ link, and $R_2^S - D_{R_x}^P$ link and I_{th} is the interference threshold power. Note that the objective function stated in equation (5.2.2) is a concave function.

Remarks on concavity of the objective function: Note that if a function $f(x)$ is assumed to be concave, then $-f(x)$ will be a convex function [145]. Therefore, to check the concavity of the function $f(\psi_S)$ in equation (5.2.2), we first check the convexity of function $-f(\psi_S)$. For the convexity analysis, the condition is that the double derivative of the function is greater than zero ($-f''(\psi_S) > 0$). If this condition satisfies, then $-f(\psi_S)$ is convex, which in turn proves that $f(\psi_S)$ is concave. Therefore, if convex function $-f(\psi_S)$ is,

$$-f(\psi_S) = -p_1 \log_2(1 + \mathbb{F}_1\psi_S) - p_2 \log_2(1 + \mathbb{F}_2\psi_S), \quad (5.2.4)$$

where $\mathbb{F}_1 = \frac{P_r\gamma_{r_1d}^s}{\sigma_d^2 d^\nu}$ and $\mathbb{F}_2 = \frac{P_r\gamma_{r_2d}^s}{\sigma_d^2 d^\nu}$, then the double derivative of equation (5.2.4) is

$$-f''(\psi_S) = p_1 \frac{\mathbb{F}_1^2}{(\mathbb{F}_1\psi_S + 1)^2} + p_2 \frac{\mathbb{F}_2^2}{(\mathbb{F}_2\psi_S + 1)^2} > 0. \quad (5.2.5)$$

Therefore, it can be analyzed that $-f(\psi_S)$ is convex, hence $f(\psi_S)$ is concave. Further, reformulate the concave function into a convex optimization problem by negating the objective function in (5.2.2) and solving it to obtain ψ_S^* .

Result 19 Optimal FASE relaying policy: *The optimal RGF that maximizes FASE is a unique positive solution of the following quadratic equation:*

$$A\psi_S^2 + B\psi_S + C = 0, \quad (5.2.6)$$

where

$$\begin{aligned} A &= \frac{P_r\gamma_{r_1d}^s}{\sigma_d^2 d^\nu} \times \frac{P_r\gamma_{r_2d}^s}{\sigma_d^2 d^\nu} \times \left[\frac{\mathcal{M}P_r(p_1\gamma_{r_1d}^i + p_2\gamma_{r_2d}^i) \ln(2)}{\sigma_D^2 D^\nu} \right], \\ B &= \left[\frac{P_r(\gamma_{r_1d}^s + \gamma_{r_2d}^s)}{\sigma_d^2 d^\nu} \right] \times \left[\frac{\mathcal{M}P_r(p_1\gamma_{r_1d}^i + p_2\gamma_{r_2d}^i) \ln(2)}{\sigma_D^2 D^\nu} \right] - \left[\frac{P_r\gamma_{r_1d}^s}{\sigma_d^2 d^\nu} \times \frac{P_r\gamma_{r_2d}^s}{\sigma_d^2 d^\nu} \right], \\ C &= \left[\frac{\mathcal{M}P_r(p_1\gamma_{r_1d}^i + p_2\gamma_{r_2d}^i) \ln(2)}{\sigma_D^2 D^\nu} \right] - \left[\frac{P_r(p_1\gamma_{r_1d}^s + p_2\gamma_{r_2d}^s)}{\sigma_d^2 d^\nu} \right]. \end{aligned}$$

The optimal solution is the unique positive root of equation (5.2.6). Further, $\mathcal{M} > 0$ is the Lagrange multiplier and is set such that it should satisfy the average interference constraint defined in equation (5.2.3). The proof of the above result is relegated in

Appendix D.1

Remarks on power conservation rule for optimal FASE relaying policy: We state the following power conservation rule to avoid transmissions in poor channel conditions. It states that if the link quality is not good between the selected relay and the destination node, the relay should stay idle and do not process and forward its received signal to the SU destination. Mathematically, $\left[\frac{\mathcal{M}Pr(p_1\gamma_{r_1d}^i + p_2\gamma_{r_2d}^i) \ln(2)}{\sigma_D^2 D^\nu} \right] - \left[\frac{Pr(p_1\gamma_{r_1d}^s + p_2\gamma_{r_2d}^s)}{\sigma_d^2 d^\nu} \right] < 0$ for $\psi_S^* = 0$. After rearranging, we have

$$\gamma_{r_2d}^s < \beta \triangleq \frac{\mathcal{M}(p_1\gamma_{r_1d}^i + p_2\gamma_{r_2d}^i) \ln(2) \sigma_d^2 d^\nu - p_1\gamma_{r_1d}^s \sigma_D^2 D^\nu}{p_2\sigma_D^2 D^\nu}. \quad (5.2.7)$$

Result 20 Exact optimal FASE expression: *The exact analytical expression for FASE is as follows:*

$$\bar{\mathcal{S}} = \mathbb{X} \left[\int_{\gamma_{r_2d}^i=0}^{\infty} \int_{\gamma_{r_1d}^i=0}^{\infty} \int_{\gamma_{r_1d}^s=0}^{\infty} \int_{\gamma_{r_2d}^s=\beta}^{\infty} \left[p_1 \log_2 \left(1 + \mathbb{Y}_1 \gamma_{r_1d}^s \right) + p_2 \log_2 \left(1 + \mathbb{Y}_1 \gamma_{r_2d}^s \right) \right] \mathbb{Z} d\gamma_{r_2d}^s d\gamma_{r_1d}^s d\gamma_{r_1d}^i d\gamma_{r_2d}^i \right], \quad (5.2.8)$$

where $\mathbb{X} = \frac{1}{\bar{\gamma}_{r_1d}^s \bar{\gamma}_{r_2d}^s \bar{\gamma}_{r_1d}^i \bar{\gamma}_{r_2d}^i}$, $\mathbb{Y}_1 = \frac{\psi_S^* Pr}{\sigma_d^2 d^\nu}$, and $\mathbb{Z} = e^{-\frac{\gamma_{r_1d}^s}{\bar{\gamma}_{r_1d}^s}} \times e^{-\frac{\gamma_{r_2d}^s}{\bar{\gamma}_{r_2d}^s}} \times e^{-\frac{\gamma_{r_1d}^i}{\bar{\gamma}_{r_1d}^i}} \times e^{-\frac{\gamma_{r_2d}^i}{\bar{\gamma}_{r_2d}^i}}$. Further, $\bar{\gamma}_{r_1d}^s$, $\bar{\gamma}_{r_2d}^s$, $\bar{\gamma}_{r_1d}^i$, and $\bar{\gamma}_{r_2d}^i$ is the average channel power gain of $R_1^S - D_{Rx}^S$ link, $R_2^S - D_{Rx}^S$ link, $R_1^S - D_{Rx}^P$ link and $R_2^S - D_{Rx}^P$ link respectively. A four integral expression is derived for the exact optimal FASE. We can further simplify this expression numerically. Proof of the result is relegated in Appendix D.2.

Result 21 Optimal FASE upper bound expression: *To derive the upper bound of optimal FASE expression, we use Jensen's inequality. Therefore, the expression for the upper bound FASE is given by*

$$\bar{\mathcal{S}}_{UB} = p_1 \log_2 \left(1 + \left[\mathbb{X} \int_{\gamma_{r_2d}^i=0}^{\infty} \int_{\gamma_{r_1d}^i=0}^{\infty} \int_{\gamma_{r_1d}^s=0}^{\infty} \int_{\gamma_{r_2d}^s=\beta}^{\infty} \mathbb{Y}_1 \gamma_{r_1d}^s \mathbb{Z} d\gamma_{r_2d}^s d\gamma_{r_1d}^s d\gamma_{r_1d}^i d\gamma_{r_2d}^i \right] \right) + p_2 \log_2 \left(1 + \left[\mathbb{X} \int_{\gamma_{r_2d}^i=0}^{\infty} \int_{\gamma_{r_1d}^i=0}^{\infty} \int_{\gamma_{r_1d}^s=0}^{\infty} \int_{\gamma_{r_2d}^s=\beta}^{\infty} \mathbb{Y}_1 \gamma_{r_2d}^s \mathbb{Z} d\gamma_{r_2d}^s d\gamma_{r_1d}^s d\gamma_{r_1d}^i d\gamma_{r_2d}^i \right] \right). \quad (5.2.9)$$

A four integral expression is derived for the upper bound optimal FASE. We can further simplify this expression numerically. Proof of the result is relegated in Appendix D.3.

Remarks: The exact optimal FASE and its upper bound contain the same number of integrals, which we evaluate numerically. However, the upper bound is useful to develop asymptotic analysis in a scaling regime.

5.2.2 Optimal FAEE of IC-PA-DAF

In this section, we analyze the FAEE of the energy efficient IC-PA-DAF policy. This analysis will help us quantify the energy efficiency performance of the policy. Note that the energy efficient IC-PA-DAF relay set transmit power and gain to optimize FAEE. We formulate the FAEE optimization problem as follows.

$$\max_{\psi_{\mathcal{E}}} \mathbf{E} \left[\frac{\mathcal{S}}{P_{\text{total}}} \right], \quad (5.2.10)$$

$$\text{s.t. } \mathbf{E} \left[p_1 \frac{\psi_{\mathcal{E}} P_r \gamma_{r1d}^i}{\sigma_D^2 D^\nu} + p_2 \frac{\psi_{\mathcal{E}} P_r \gamma_{r2d}^i}{\sigma_D^2 D^\nu} \right] \leq I_{\text{th}}, \quad (5.2.11)$$

where P_{total} is the total power consumed in the C-SSS. Mathematically, we have

$$P_{\text{total}} = P_s + P_c + \psi_{\mathcal{E}} P_r. \quad (5.2.12)$$

where P_s is the source transmit power, P_c is the power consumed by the circuitry, and P_r is the relay transmit power. Note that the relays used in the network are IC-PA-DAF relays. Hence, the transmit power of the relay will be $\psi_{\mathcal{E}} P_r$.

Substituting the expression for spectral efficiency and P_{total} in equation (5.2.10), we get

$$\max_{\psi_{\mathcal{E}}} \mathbf{E} \left[\frac{p_1 \log_2 \left(1 + \frac{\psi_{\mathcal{E}} P_r \gamma_{r1d}^s}{\sigma_a^2 d^\nu} \right) + p_2 \log_2 \left(1 + \frac{\psi_{\mathcal{E}} P_r \gamma_{r2d}^s}{\sigma_a^2 d^\nu} \right)}{P_s + P_c + \psi_{\mathcal{E}} P_r} \right], \quad (5.2.13)$$

$$\text{s.t. } \mathbf{E} \left[p_1 \frac{\psi_{\mathcal{E}} P_r \gamma_{r1d}^i}{\sigma_D^2 D^\nu} + p_2 \frac{\psi_{\mathcal{E}} P_r \gamma_{r2d}^i}{\sigma_D^2 D^\nu} \right] \leq I_{\text{th}}. \quad (5.2.14)$$

As can be observed, the FAEE optimization problem is concave. To obtain the optimized $\psi_{\mathcal{E}}$, we convert the concave optimization problem to convex and solve it.

Result 22 Optimal FAEE relaying policy: *The optimal RGF that maximizes FAEE*

is a unique positive solution of the following transcendental equation:

$$\begin{aligned} \frac{\mathcal{M}'(p_1\gamma_{r_1d}^i + p_2\gamma_{r_2d}^i) \ln(2)}{\sigma_D^2 D^\nu} &= \left[\frac{p_1\gamma_{r_1d}^s}{(\sigma_d^2 d^\nu + \psi_\varepsilon P_r \gamma_{r_1d}^s)(P_{sc} + \psi_\varepsilon P_r)} - \frac{p_1 \ln\left(1 + \frac{\psi_\varepsilon P_r \gamma_{r_1d}^s}{\sigma_d^2 d^\nu}\right)}{(P_{sc} + \psi_\varepsilon P_r)^2} \right] \\ &+ \left[\frac{p_2\gamma_{r_2d}^s}{(\sigma_d^2 d^\nu + \psi_\varepsilon P_r \gamma_{r_2d}^s)(P_{sc} + \psi_\varepsilon P_r)} - \frac{p_2 \ln\left(1 + \frac{\psi_\varepsilon P_r \gamma_{r_2d}^s}{\sigma_d^2 d^\nu}\right)}{(P_{sc} + \psi_\varepsilon P_r)^2} \right], \end{aligned} \quad (5.2.15)$$

where $P_{sc} = P_s + P_c$. Solving the above transcendental equation numerically, we get the optimal solution. The proof of the result is shown in Appendix D.4.

Further, we state the power conservation rule for optimal FAEE policy.

Remarks on power conservation rule for optimal FAEE relaying policy: This rule states that the relay should refrain itself from transmitting the signal and should conserve its power. This rule applies in the situation when the channel condition between selected IC-PA-DAF relay to destination link is not good. Furthermore, we can mathematically write this rule as $\psi_\varepsilon^* = 0$ if $p_1\left(\frac{\gamma_{r_1d}^s}{(\sigma_d^2 d^\nu)(P_{sc})}\right) + p_2\left(\frac{\gamma_{r_2d}^s}{(\sigma_d^2 d^\nu)(P_{sc})}\right) - \frac{\mathcal{M}'(p_1\gamma_{r_1d}^i + p_2\gamma_{r_2d}^i) \ln(2)}{\sigma_D^2 D^\nu} < 0$. This can be rearranged further and can be written as

$$\gamma_{r_2d}^s < \beta' \triangleq \frac{\mathcal{M}'\sigma_d^2 d^\nu P_{sc}(p_1\gamma_{r_1d}^i + p_2\gamma_{r_2d}^i) \ln(2)}{p_2\sigma_D^2 D^\nu} - \frac{p_1\gamma_{r_1d}^s}{p_2}. \quad (5.2.16)$$

Therefore, based on the power conservation rule and optimum RGF, the FAEE for the model proposed can be derived.

Result 23 Exact optimal FAEE expression: *The exact analytical expression for optimal FAEE is as follows:*

$$\begin{aligned} \bar{\mathcal{E}} &= \left[\int_{\gamma_{r_2d}^i=0}^{\infty} \int_{\gamma_{r_1d}^i=0}^{\infty} \int_{\gamma_{r_1d}^s=0}^{\infty} \int_{\gamma_{r_2d}^s=\beta'}^{\infty} \mathbb{X} \left[\left(\frac{p_1 \log_2(1 + \mathbb{Y}_2 \gamma_{r_1d}^s)}{P_{sc} + \psi_\varepsilon^* P_r} \right) \right. \right. \\ &\quad \left. \left. + \left(\frac{p_2 \log_2(1 + \mathbb{Y}_2 \gamma_{r_2d}^s)}{P_{sc} + \psi_\varepsilon^* P_r} \right) \right] \mathbb{Z} d\gamma_{r_2d}^s d\gamma_{r_1d}^s d\gamma_{r_1d}^i d\gamma_{r_2d}^i \right], \end{aligned} \quad (5.2.17)$$

where $\mathbb{Y}_2 = \frac{\psi_\varepsilon^* P_r}{\sigma_d^2 d^\nu}$. A four integral expression is derived for the exact optimal FAEE. We can further simplify this expression numerically. Proof of the result is relegated in Appendix D.5.

The upper bound analytical expression for FAEE is as follows:

Result 24 Optimal FAEE upper bound expression: *Further using the inequality $\log_2(1+y) < y$ for $y > 0$. The upper bound expression for the optimal FAEE can be written as*

$$\bar{\mathcal{E}}_{UB} = \left[\int_{\gamma_{r_2d}^i=0}^{\infty} \int_{\gamma_{r_1d}^i=0}^{\infty} \int_{\gamma_{r_1d}^s=0}^{\infty} \int_{\gamma_{r_2d}^s=\beta'}^{\infty} \mathbb{X} \left[\left(\frac{p_1 \Upsilon_2 \gamma_{r_1d}^s}{P_{sc} + \psi_{\mathcal{E}}^* P_r} \right) + \left(\frac{p_2 \Upsilon_2 \gamma_{r_2d}^s}{P_{sc} + \psi_{\mathcal{E}}^* P_r} \right) \right] \mathbb{Z} d\gamma_{r_2d}^s d\gamma_{r_1d}^s d\gamma_{r_1d}^i d\gamma_{r_2d}^i \right]. \quad (5.2.18)$$

A four integral expression is derived for the upper bound FAEE. We can evaluate the upper bound optimal FAEE numerically. The proof of the result is relegated in Appendix D.6.

Further, in the next section, we present the numerical results for the expressions derived for the proposed model.

5.3 Numerical Results and Benchmarking for N-EH C-SSS Model

Table 5.1: Simulation parameters for N-EH relay-assisted C-SSS model.

Simulation parameter	Symbol	Value
Number of channel realization	N	10^5
Mean channel power gain	$\bar{\gamma}_{r_{nd}}^s$ and $\bar{\gamma}_{r_{nd}}^i$ ($n \in 1, 2$)	1
Noise variance	σ_d^2 and σ_D^2	1
Threshold interference power	I_{th}	15 dB
Source transmit power	P_s	P_s = relay transmit power before power adaptation
Power consumed by the circuitry	P_c	15 dBm
Secondary source node to relay node distance	d	1 m
Relay node to primary destination distance	D	1 m
Path loss exponent	ν	2.7 [100]
Symbol energy	$ x ^2$	1 [38]

In this section, we numerically evaluate the performance of IC-PA-DAF relaying policy adopted with PRSP in underlay C-SSS. To validate the derived expressions,

we perform Monte-Carlo simulations. Table 5.1 shows the simulation parameters used for generating the results. However, simulation specific parameters are briefly described inside the captions of the simulation results. To gain quantitative insights into the proposed system and policy, we use benchmark policies for performance comparison. For a fair comparison, we consider simple regenerative (DAF) relaying policy jointly with PRSP, and fixed gain DAF relaying policy together with PRSP. Note that the transmit power of relay in both the benchmark policies is constrained to avoid interference [93].

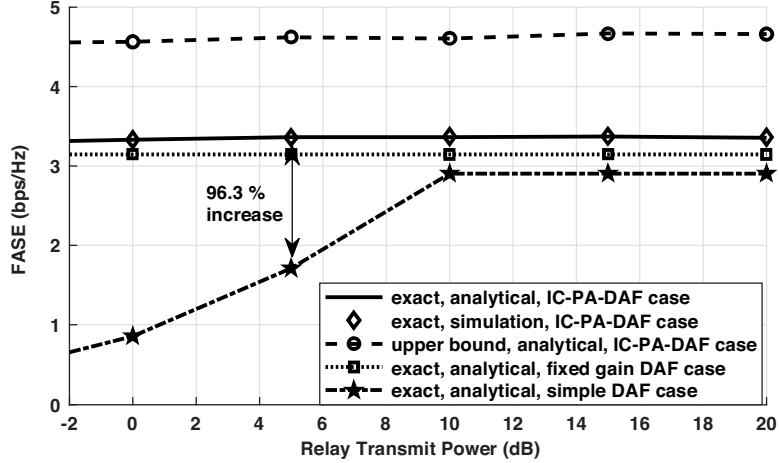


Figure 5.2: FASE as a function of relay transmit power ($I_{\text{th}} = 10$ dB, mean channel power gain = 1 (for all links), $d = 1\text{m}$, $D = 1\text{m}$, $\nu = 2.7$, $\sigma_d^2 = 1$, $\sigma_D^2 = 1$).

Figure 5.2 plots exact optimal FASE, its upper bound, and the FASE of benchmark policies, as a function of relay transmit power. We see that the proposed IC-PA-DAF policy outperforms the benchmark policies in terms of FASE. We see that the proposed policy delivers a 96.3% improvement compared to the simple DAF policy. The flat nature of the curves is due to the average interference-constraint. Furthermore, the upper bound of optimal FASE, though not tight, track the exact plot well.

Figure 5.3 plots the exact optimal FASE, its upper bound and FASE of the benchmark policies as a function of mean channel power gain. As evident, with the increase in mean channel power gain, all case's spectral efficiency increases, as expected. Furthermore, the proposed IC-PA-DAF policy delivers superior performance in terms of FASE. This superior performance is due to the CSI aware power-adaptation by the proposed policy.

Figure 5.4 plots the exact optimal FAEE, its upper bound, and the benchmark policies FAEE as a function of relay transmit power. We observe that as transmit power increases, the power consumption of the system model increases. Therefore,

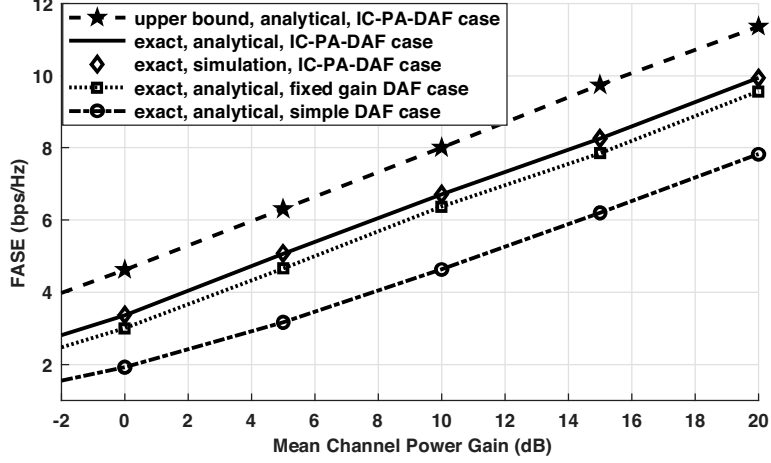


Figure 5.3: FASE as a function of mean channel power gain ($I_{\text{th}} = 10$ dB, $P_r = 6$ dB, $d = 1$ m, $D = 1$ m, $\nu = 2.7$, $\sigma_d^2 = 1$ and $\sigma_D^2 = 1$).

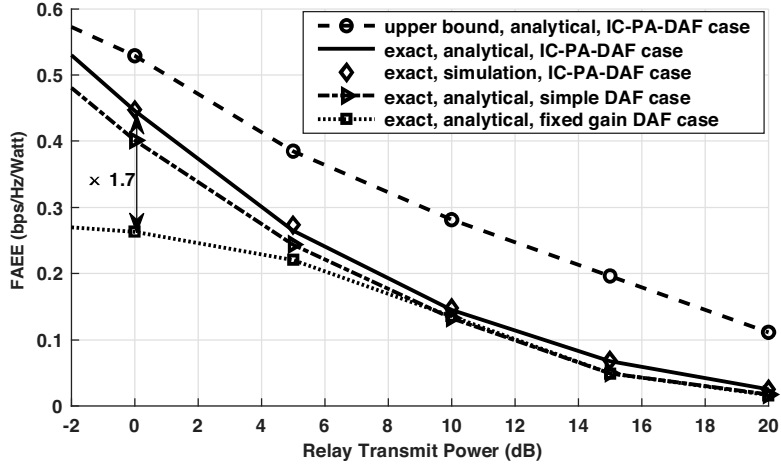


Figure 5.4: FAEE as a function of relay transmit power ($I_{\text{th}} = 10$ dB, $P_c = 15$ dBm, mean channel power gain = 1 (for all links), $d = 1$ m, $D = 1$ m, $\nu = 2.7$, $\sigma_d^2 = 1$, $\sigma_D^2 = 1$).

the energy efficiency of the system decreases. Furthermore, due to the IC-PA-DAF policy's adaptive nature, the proposed policy performs better than the benchmark policies. For the proposed policy, the upper bound tracks the optimal FAEE well.

5.4 EH Relay-Assisted C-SSS Model

Figure 5.5 depicts the green underlay cooperative spectrum sharing wireless communication system model. In the proposed system model, the secondary cloud contains all the SUs, whereas nodes outside the secondary cloud are PUs. In the secondary cloud, the secondary source node S_{Tx}^s strives to transmit the information signal (α) to the secondary destination node D_{Rx}^s . It is important to note that for the system

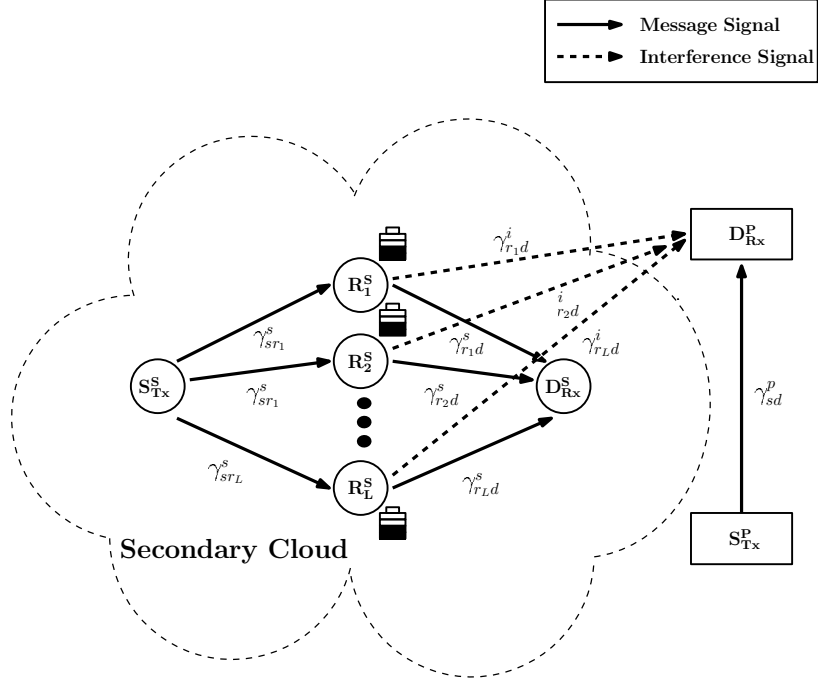


Figure 5.5: EH based IC-PA-DAF relay-assisted C-SSS.

model considered, we assume that the S_{Tx}^s node is not in the transmission range of the D_{Rx}^s node. Therefore, the cooperating secondary relay nodes R_n^s (where $n \in 1, 2, \dots, L$) assist the S_{Tx}^s node in forwarding the signal to the D_{Rx}^s node. Further, it is assumed that the relays have RF-EH capability and use the harvested energy to forward the signal to the destination.

In order to decrease the implementation complexity of the system model, we incline towards adopting a relay selection policy. The selection of secondary relay nodes (R_s^s) is based on EH based relay selection (EHRS) policy. Furthermore, we assume that all the nodes inside and outside the secondary cloud have a single RF antenna for transmission and reception. Additionally, all the channels of the system model are assumed to be statistically independent and frequency flat Rayleigh fading channels. We also assume that all the signal transmission takes place on the same bandwidth, and all the relays are half-duplex. Lastly, the source node and the destination node inside and outside the secondary cloud are not power constrained and have sufficient energy resources.

It is assumed that the known pilot sequences-based estimation protocols are used for CSI acquisition by the R_s^s relay node. In the system model, IC-PA-DAF relays are used to assist the S_{Tx}^s . The acquisition of CSI is essential since these relays adaptively set their transmit power and gain to forward the signal to the D_{Rx}^s .

Remarks on IC-PA-DAF relays: IC-PA-DAF relay nodes are hybrid relay nodes since these nodes simultaneously perform both amplification and decoding tasks be-

fore forwarding the encoded signal to D_{Rx}^{s} . In IC-PA-DAF relays, the amplification performed by the relay is adaptive, and is based on RGF φ_x (where, $x \rightarrow \mathcal{S}$ for optimizing FASE, and $x \rightarrow \mathcal{E}$ for optimizing FAEE). It is important to note that the RGF is based on the channel power gain of three links, which are, $S_{\text{Tx}}^{\text{s}} - R_{\text{S}}^{\text{s}}$ link ($\gamma_{\text{max}}^{\text{s}}$), $R_{\text{S}}^{\text{s}} - D_{\text{Rx}}^{\text{s}}$ link ($\gamma_{r_{\text{s}d}}^{\text{s}}$), and $R_{\text{S}}^{\text{s}} - D_{\text{Rx}}^{\text{p}}$ link ($\gamma_{r_{\text{s}d}}^{\text{i}}$). Therefore, when the selected relay receives the signal, it decodes, re-encodes, and amplifies (based on φ_x) the signal before forwarding it to the D_{Rx}^{s} . Furthermore, the transmit power of the selected IC-PA-DAF relay is interference-constrained, that is, the transmit power of the relay cannot exceed the interference threshold (I_{th}). This interference constraint helps in avoiding the interference at D_{Rx}^{p} created by R_{S}^{s} .

Note: In this chapter, we independently propose the optimization problems for FASE and FAEE to derive optimized RGF for both of them. Hence the RGF derived for optimizing FASE need not optimize FAEE and vice versa. Furthermore, for better clarity, the RGF to optimize FASE will be denoted by ($\varphi_{\mathcal{S}}$), and the RGF to optimize FAEE will be denoted by ($\varphi_{\mathcal{E}}$). Lastly, using these RGF $\varphi_{\mathcal{S}}$ and $\varphi_{\mathcal{E}}$, the exact and upper bound expressions for FASE and FAEE are derived, respectively.

Remarks on RF-EH: The relay nodes cooperating with S_{Tx}^{s} to forward the signal have RF-EH capabilities. Therefore, the signal received by the relay nodes from S_{Tx}^{s} will also be used to harvest energy. Further, harvested energy will be used to forward the signal to the destination. TSP is adopted for SWIPT between S_{Tx}^{s} and all the relays. Note that the residual energy harvested by the non selected relays for each T time slot will be used for data transmission to other destinations.

5.4.1 Transmission Protocol

Transmission of the data symbol α (having unit energy) from S_{Tx}^{s} node to D_{Rx}^{s} node takes place in two phases: i.) Broadcasting phase and ii.) Forwarding Phase. In the following points, we discuss both phases briefly.

- *Broadcasting Phase:* In this phase, the source node S_{Tx}^{s} broadcasts the information signal to the relay nodes present in the secondary cloud. The transmit power of the broadcasted information signal is denoted by P_s .
- *Forwarding Phase:* In this phase, initially, all the relay nodes harvest energy from the signal received via S_{Tx}^{s} . The relay node selected for information transmission based on EHRS policy further uses the harvested energy to forward the signal to the D_{Rx}^{s} node. However, before forwarding the signal, the received information signal is first decoded, then re-encoded, and lastly amplified based on

optimal φ_x . This is done since the relays considered in the system model are IC-PA-DAF relays. Furthermore, the optimal φ_x is adaptive and is dependent on γ_{\max}^s , $\gamma_{r_{sd}}^s$, and $\gamma_{r_{sd}}^i$ channel power gains. It is important to note that the transmit power of the selected relay is interference-constrained to avoid interference at $D_{R_x}^p$ since underlay C-SSS is considered.

5.4.2 Remarks on TSP

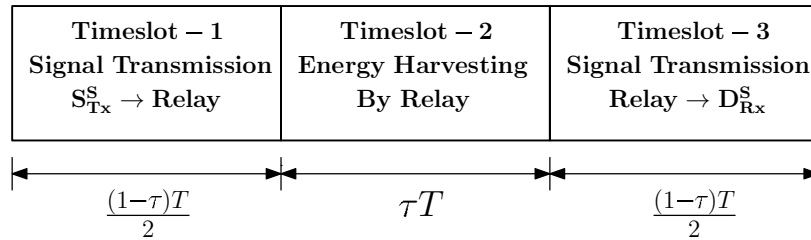


Figure 5.6: Illustration of timeslots in TSP.

TSP contains two crucial tasks, that are, i.) signal transmission, and ii.) energy harvesting. Figure 5.6 illustrates the timeslots of TSP where T represents the block time for complete transmission of symbol from S_{Tx}^s to D_{Rx}^s and τ represents energy harvesting duty cycle. Timeslot - 1 of duration $\left(\frac{(1-\tau)T}{2}\right)$ represents the time required for the transmission of the signal from the secondary source to the secondary relay. Timeslot - 2 of duration (τT) represents the RF-EH duration of the secondary relay. Lastly, Timeslot - 3 of duration $\left(\frac{(1-\tau)T}{2}\right)$ represents the time required for the transmission of the signal from the secondary relay to the secondary destination.

5.4.3 Remarks on CSI

Following are the CSI requirements of the IC-PA-DAF relay-assisted green underlay C-SSS.

- *Secondary source S_{Tx}^s CSI requirement:* The source node S_{Tx}^s is responsible for the selection of the best relay based on the EHRS policy. Therefore, for determining the relay that harvests the maximum energy, S_{Tx}^s requires instantaneous CSI information of itself to all the relay nodes in the secondary cloud. For acquiring the CSI, the pilot sequence can be sent to the relay nodes by S_{Tx}^s , and in response (by virtue of channel reciprocity), the estimated CSI is received back to the source node from all the relay nodes. However, this technique is not suitable for the energy-constrained system model. Therefore, a more suitable CSI acquisition technique is a one-bit feedback algorithm proposed in [127].

- *Relay node CSI requirement:* Initially, the relay node R_S^s selected to cooperate with the S_{Tx}^s node requires instantaneous CSI of link between the source node and itself to decode the received signal. Further, since IC-PA-DAF relay nodes are employed, the signal to be forwarded is re-encoded and amplified adaptively. Therefore, for adaptive amplification of the signal, the relay requires instantaneous CSI of $S_{Tx}^s - R_S^s$ link, $R_S^s - D_{Rx}^s$ link, and $R_S^s - D_{Rx}^p$ link.
- *Secondary destination D_{Rx}^s node:* The secondary destination node only requires instantaneous CSI of the R_S^s relay to the D_{Rx}^s link. This CSI information is required to decode the signal received by the D_{Rx}^s node from R_S^s .
- *Primary node CSI requirement:* The primary source node S_{Tx}^p directly transmits its information signal to the primary destination node D_{Rx}^p . Therefore, only D_{Rx}^p requires CSI of the $S_{Tx}^p - D_{Rx}^p$ link to decode the signal received from S_{Tx}^p .

5.4.4 Remarks on complexity aspects while employing multiple relays

Increasing the number of relays for C-SSS will increase the complexity at the SU source node responsible for the relay selection. However, there is a trade-off between complexity and the performance of the proposed system. The selection of the appropriate relay for signal transmission to the destination has the following advantages.

- *Reduced hardware complexity and processing at the relay:* The best relay selection reduces the required number of RF chains, and hence, processing complexity [47].
- *Reduced problem of synchronization at the destination:* Relay selection is of practical interest because it avoids the tight synchronization required among multiple transmitting relays [48].
- *Improved energy efficiency of the overall system:* Relay selection reduces the processing burden on multiple relay RF chains, which decreases overall power consumption. Therefore, energy efficiency, which is the ratio of spectral efficiency per unit power consumption, increases.

Furthermore, there are various use cases where multiple relays are helpful. Following are some examples.

- *Cooperative vehicular communications:* Consider the use case in a cognitive inter-vehicular cooperative system [146] where we need the multiple relays (example, road-side units) to be placed at the strategic locations and employ relay selection to enhance reliable transmission range.
- *Unmanned aerial vehicle (UAV) selection in C-SSS:* A drone or UAV-assisted cooperative spectrum sharing network [147] could employ a drone selection policy to improve end-to-end network performance. Consider a use case where the source and the destination nodes are significantly apart. In it, multiple UAVs can be deployed to enhance the reliable transmission range. In such a drone-assisted C-SSS, the selected UAV could forward its received signal to the destination based on the relaying policy.

Lastly, mobile edge computing (MEC) techniques which have recently gained so much popularity due to their advantages, can be employed in the system model. In the MEC technique, the secondary source node can off-load its computational tasks to the specialized access points within proximity for executing the task remotely. Furthermore, by incorporating the MEC techniques [148, 149], it is possible to reduce the source node processing burden and computational complexity in a C-SSS.

5.4.5 Remarks on EHRS

In this chapter, we opt for an EHRS policy. EHRS policy is a partial relay selection policy. In this policy, the source node selects the best relay based on the energy harvesting criteria. Therefore, the relay which harvests maximum energy is selected to forward the signal to the D_{Rx}^s . Let $\mathcal{E}\mathcal{H}_1, \mathcal{E}\mathcal{H}_2, \dots, \mathcal{E}\mathcal{H}_L$ denote the energy harvested by L relay nodes. Hence, the EHRS criteria can be mathematically expressed as

$$\mathcal{H} = \arg \max_{1,2,\dots,L} \mathcal{E}\mathcal{H}_n, \quad (5.4.1)$$

where $\mathcal{E}\mathcal{H}_n = \frac{\eta P_s \gamma_n^s \tau T}{d_s^\nu}$, P_s is the source transmit power, η is the energy conversion efficiency, γ_n^s is the channel power gain of the S_{Tx}^s to n^{th} relay link, d_s is the distance between the S_{Tx}^s to the relay node, and ν is the path loss exponent. Further, the maximum harvested energy by the relay node can be expressed as

$$\mathcal{E}\mathcal{H}_{\max} = \max\{\mathcal{E}\mathcal{H}_1, \mathcal{E}\mathcal{H}_2, \dots, \mathcal{E}\mathcal{H}_L\}. \quad (5.4.2)$$

Taking constant terms outside, the above equation can be written as

$$\mathcal{E}\mathcal{H}_{\max} = k \times \gamma_{\max}^s. \quad (5.4.3)$$

where $k = \frac{\eta P_s \tau T}{d_s^\nu}$, and $\gamma_{\max}^s \triangleq \max\{\gamma_1^s, \gamma_2^s, \dots, \gamma_L^s\}$. Furthermore, the pdf of γ_{\max}^s can be expressed as [115]

$$p_{\mathcal{E}\mathcal{H}_{\max}}(\gamma_{\max}^s) = \frac{L}{\bar{\gamma}_{\max}^s} \exp\left(-\frac{\gamma_{\max}^s}{\bar{\gamma}_{\max}^s}\right) \left(1 - \exp\left(-\frac{\gamma_{\max}^s}{\bar{\gamma}_{\max}^s}\right)\right)^{L-1}, \quad (5.4.4)$$

where L is the number of relay nodes in the system and $\bar{\gamma}_{\max}^s$ is the average channel power gain of the link between the secondary source to the relay, which harvests maximum energy. We use the above pdf while deriving the optimized FASE and FAEE of the proposed system model.

In the following section, we will be formulating the problem statement to enhance spectral efficiency and energy efficiency independently by optimizing RGF. By independently we mean that the optimized RGF used to derive enhanced spectral efficiency cannot be used to enhance energy efficiency and vice versa.

5.5 Optimization and Analysis for EH C-SSS

In this section, we consider the performance measures independently. For each performance measure, we first define the problem statement to enhance the performance measure based on the optimized φ_x . We then solve the problem statement to obtain the optimized φ_x . Once the optimized φ_x is obtained, we then derive the exact and the upper bound expression for the performance measure considered. For the analysis, we have considered the two most crucial performance measures, that is, FASE and FAEE. To analyze these performance measures, we first express the SNR at the secondary destination. Let Γ_D be the end SNR at the secondary destination node D_{Rx}^s . Therefore, mathematically it is written as

$$\begin{aligned} \Gamma_D &= \frac{\varphi_x(\gamma_{\max}^s, \gamma_{r_{sd}}^s, \gamma_{r_{sd}}^i) \max\{\mathcal{E}\mathcal{H}_1, \mathcal{E}\mathcal{H}_2, \dots, \mathcal{E}\mathcal{H}_L\} \gamma_{r_{sd}}^s}{\sigma_{D_s}^2 D_s^\nu}, \\ &= \frac{k \varphi_x(\gamma_{\max}^s, \gamma_{r_{sd}}^s, \gamma_{r_{sd}}^i) \max\{\gamma_1, \gamma_2, \dots, \gamma_L\} \gamma_{r_{sd}}^s}{\sigma_{D_s}^2 D_s^\nu}, \end{aligned} \quad (5.5.1)$$

where $\varphi_x(\gamma_{\max}^s, \gamma_{r_{sd}}^s, \gamma_{r_{sd}}^i)$ is the RGF which is dependent on the channel power gain of $S_{\text{Tx}}^s - R_{\text{S}}^s$ link (γ_{\max}^s), $R_{\text{S}}^s - D_{\text{Rx}}^s$ link ($\gamma_{r_{sd}}^s$) and $R_{\text{S}}^s - D_{\text{Rx}}^p$ link ($\gamma_{r_{sd}}^i$), D_s is the length of $R_{\text{S}}^s - D_{\text{Rx}}^s$ link, and $\sigma_{D_s}^2$ is noise variance.

Assuming, $\gamma_{\max}^s \triangleq \max\{\gamma_1, \gamma_2, \dots, \gamma_L\}$, and $C_1 = \frac{k}{\sigma_{d_s}^2 D_s^\nu}$. Therefore, the above equation can be written as

$$\Gamma_D = C_1 \varphi_x(\gamma_{\max}^s, \gamma_{r_{sd}}^s, \gamma_{r_{sd}}^i) \gamma_{\max}^s \gamma_{r_{sd}}^s. \quad (5.5.2)$$

Below, we present the optimization problem statement and derive the optimal solution of FASE and FAEE.

5.5.1 Optimal Relaying Policy for FASE and Its Analysis

For the system model considered, FASE gives information regarding the information rate that a system model can achieve. To analyze FASE, the instantaneous spectral efficiency is averaged with respect to the fading channel. The FASE of the system model can be expressed as

$$\bar{\mathcal{S}} = \mathbf{E}[\log_2(1 + \Gamma_D)]. \quad (5.5.3)$$

Further, we define the optimization problem to derive the optimum RGF, which can enhance the spectral efficiency of the system model.

Optimization problem: To obtain the expression for enhanced FASE, we first define the problem statement. Therefore the problem statement can be expressed as

$$\max_{\varphi_S(\gamma_{\max}^s, \gamma_{r_{sd}}^s, \gamma_{r_{sd}}^i)} \mathbf{E} \left[\log_2(1 + C_1 \varphi_S(\gamma_{\max}^s, \gamma_{r_{sd}}^s, \gamma_{r_{sd}}^i) \gamma_{\max}^s \gamma_{r_{sd}}^s) \right], \quad (5.5.4)$$

$$\text{s.t. } \mathbf{E} \left[C_2 \varphi_S(\gamma_{\max}^s, \gamma_{r_{sd}}^s, \gamma_{r_{sd}}^i) \gamma_{\max}^s \gamma_{r_{sd}}^i \right] \leq I_{\text{th}}, \quad (5.5.5)$$

where $C_2 = \frac{2\eta P_s \tau}{(1-\tau)d_s^\nu \mathcal{D}_i^\nu}$, and \mathcal{D}_i is the distance between the secondary relay to the primary destination. For ease of representation, we write $\varphi_S(\gamma_{\max}^s, \gamma_{r_{sd}}^s, \gamma_{r_{sd}}^i)$ as φ_S in the rest of the chapter. Further, we present the result for the optimal RGF to optimize FASE.

Result 25 Optimal relay gain function for FASE: *The RGF function that maximizes FASE is a unique positive solution of the following equation.*

$$\varphi_S^* = \frac{C_1 \gamma_{r_{sd}}^s - \mathcal{M} C_2 \gamma_{r_{sd}}^i \ln(2)}{\mathcal{M} C_1 C_2 \gamma_{r_{sd}}^i \gamma_{r_{sd}}^s \gamma_{\max}^s \ln(2)}, \quad (5.5.6)$$

where $\mathcal{M} > 0$ is the Lagrange multiplier, and its value is set such that the average interference constraint in equation (5.5.5) should be satisfied. Further, the above equation is the optimum expression for RGF φ_S , which enhances fading averaged spectral efficiency. The proof of this result is relegated in Appendix D.7.

Power conservation rule: We state the following rule to conserve the power of the proposed relay. As per power conservation rule, we have, $\varphi_S^* = 0$ for $C_1 \gamma_{r_{sd}}^s < \mathcal{M} C_2 \gamma_{r_{sd}}^i \ln(2)$. This rule implies, if the channel quality between the relay and the secondary destination is not good, in that case, the relay will restrict itself from the

signal transmission. Hence the relay conserve energy. Furthermore, after rearranging the above equation, we get

$$\rho(\gamma_{r_{sd}}^i) \triangleq \gamma_{r_{sd}}^s \leq \frac{\mathcal{M}C_2\gamma_{r_{sd}}^i \ln(2)}{C_1}. \quad (5.5.7)$$

Result 26 Exact expression for FASE: *The exact analytical FASE's expression is shown below*

$$\bar{\mathcal{S}} = \log_2 \left(1 + \frac{C_1 \bar{\gamma}_{r_{sd}}^s}{\mathcal{M}C_2 \bar{\gamma}_{r_{sd}}^i} \right), \quad (5.5.8)$$

where $\bar{\gamma}_{r_{sd}}^s$, and $\bar{\gamma}_{r_{sd}}^i$ are the mean channel power gain of $R_{\mathbb{S}}^s - D_{\text{Rx}}^s$ link, and $R_{\mathbb{S}}^s - D_{\text{Rx}}^p$ link, respectively. Furthermore, a closed-form expression is obtained for the exact analytical expression of FASE. The proof of the result is presented in Appendix D.8.

Remarks on the FASE expression: The FASE of the system model does not rely on the number of relays (that is, L) deployed in the secondary cloud, as shown by the result on the exact FASE. This trend is non-intuitive and conveys that the spectral efficiency of the system model will remain unchanged with the decrease or increase in the number of relays in the system model. Furthermore, similar deductions can be made for the source transmit power P_s term also. The non-dependency of the FASE on L and P_s is due to the power adaptive nature of the IC-PA-DAF relaying policy.

Further, in the following sub-section, we present the problem statement to obtain the optimized RGF that enhances energy efficiency. Based on the optimized RGF, we derive optimized FAEE expression and its upper bound for the system model considered.

5.5.2 Optimal Relaying Policy for FAEE and Its Analysis

In this section, we analyze the FAEE and its upper bound expression. FAEE is a critical performance measure to understand the utilization of the energy resources by the proposed system model. FAEE is very closely related to the performance measure analyzed in the previous section. The FAEE of the system model considered can be represented as

$$\bar{\mathcal{E}} = \mathbf{E} \left[\frac{\mathcal{S}}{P_{\text{T}}} \right], \quad (5.5.9)$$

where \mathcal{S} is the spectral efficiency, and P_{T} is the total power consumed in the network. Further, $P_{\text{T}} = P_s + P_c + P_r$, where P_c is the power consumed by the circuitry and P_r

is the relay transmit power. Mathematically, P_r can be expressed as

$$P_r = \frac{\varphi_{\mathcal{E}}(\gamma_{\max}^s, \gamma_{r_{\text{sd}}}^s, \gamma_{r_{\text{sd}}}^i) \eta P_s \tau T \gamma_{\max}^s}{\frac{(1-\tau)T}{2} d_s^{\nu}}. \quad (5.5.10)$$

Therefore, substituting equation (5.5.2), (5.5.3), (5.5.10), in equation (5.5.9), we can represent FAEE as

$$\bar{\mathcal{E}} = \mathbf{E} \left[\frac{\log_2(1 + C_1 \varphi_{\mathcal{E}}(\gamma_{\max}^s, \gamma_{r_{\text{sd}}}^s, \gamma_{r_{\text{sd}}}^i) \gamma_{\max}^s \gamma_{r_{\text{sd}}}^s)}{(P_s + P_c) + \frac{\varphi_{\mathcal{E}}(\gamma_{\max}^s, \gamma_{r_{\text{sd}}}^s, \gamma_{r_{\text{sd}}}^i) \eta P_s \tau T \gamma_{\max}^s}{\frac{(1-\tau)T}{2} d_s^{\nu}}} \right]. \quad (5.5.11)$$

Further, we define the optimization problem to derive the optimum RGF, which can enhance the energy efficiency of the system model.

Optimization problem: To obtain the expression for the optimized FAEE, we first define the problem statement. Therefore the problem statement can be expressed as

$$\max_{\varphi_{\mathcal{E}}(\gamma_{\max}^s, \gamma_{r_{\text{sd}}}^s, \gamma_{r_{\text{sd}}}^i)} \mathbf{E} \left[\frac{\log_2(1 + C_1 \varphi_{\mathcal{E}}(\gamma_{\max}^s, \gamma_{r_{\text{sd}}}^s, \gamma_{r_{\text{sd}}}^i) \gamma_{\max}^s \gamma_{r_{\text{sd}}}^s)}{(P_s + P_c) + C_3 \varphi_{\mathcal{E}}(\gamma_{\max}^s, \gamma_{r_{\text{sd}}}^s, \gamma_{r_{\text{sd}}}^i) \gamma_{\max}^s} \right], \quad (5.5.12)$$

$$\text{s.t. } \mathbf{E} \left[C_2 \varphi_{\mathcal{E}}(\gamma_{\max}^s, \gamma_{r_{\text{sd}}}^s, \gamma_{r_{\text{sd}}}^i) \gamma_{\max}^s \gamma_{r_{\text{sd}}}^s \right] \leq I_{\text{th}}, \quad (5.5.13)$$

where $\varphi_{\mathcal{E}}(\gamma_{\max}^s, \gamma_{r_{\text{sd}}}^s, \gamma_{r_{\text{sd}}}^i)$ is the RGF to optimize FAEE, and $C_3 = \frac{2\eta P_s \tau}{(1-\tau)d_s^{\nu}}$. For ease of representation, we write $\varphi_{\mathcal{E}}(\gamma_{\max}^s, \gamma_{r_{\text{sd}}}^s, \gamma_{r_{\text{sd}}}^i)$ as $\varphi_{\mathcal{E}}$ in the rest of the chapter. Further, we present the result for the optimal RGF to optimize FAEE.

Result 27 Optimal relay gain function for FAEE: *The optimized RGF that maximizes FAEE is a unique positive solution of the following equation.*

$$\ln(2) \mathcal{M}'(C_2 \gamma_{\max}^s \gamma_{r_{\text{sd}}}^s) = \frac{C_1 \gamma_{\max}^s \gamma_{r_{\text{sd}}}^s}{(1 + C_1 \varphi_{\mathcal{E}} \gamma_{\max}^s \gamma_{r_{\text{sd}}}^s)((P_s + P_c) + C_3 \varphi_{\mathcal{E}} \gamma_{\max}^s)} - \frac{C_3 \gamma_{\max}^s \ln(1 + C_1 \varphi_{\mathcal{E}} \gamma_{\max}^s \gamma_{r_{\text{sd}}}^s)}{((P_s + P_c) + C_3 \varphi_{\mathcal{E}} \gamma_{\max}^s)^2}, \quad (5.5.14)$$

where $\mathcal{M}' > 0$ is the Lagrange multiplier, and its value is set such that the average interference constraint in equation (5.5.13) should be satisfied. Note that the above equation is transcendental and can be solved numerically. The proof of this result is relegated in Appendix D.9.

Power conservation rule: We state the following rule to conserve the power of the proposed relay. As per the power conservation rule, we have $\varphi_{\mathcal{E}}^* = 0$ for $\frac{C_1 \gamma_{\max}^s \gamma_{r_{\text{sd}}}^s}{(P_s + P_c)} \leq$

$\mathcal{M}' C_2 \gamma_{\max}^s \gamma_{r_{\text{sd}}}^i \ln(2)$. Furthermore, after rearranging, we get

$$\rho'(\gamma_{r_{\text{sd}}}^i) \triangleq \gamma_{r_{\text{sd}}}^s \leq \frac{\mathcal{M}' C_2 \gamma_{r_{\text{sd}}}^i (P_s + P_c) \ln(2)}{C_1}. \quad (5.5.15)$$

Result 28 Exact expression for FAEE: *The exact analytical FAEE's expression is shown below*

$$\begin{aligned} \bar{\mathcal{E}} = & \frac{\mathcal{R}}{\ln(2)} \int_{\gamma_{\max}^s=0}^{\infty} \int_{\gamma_{r_{\text{sd}}}^i=0}^{\infty} \int_{\gamma_{r_{\text{sd}}}^s=\rho'(\gamma_{r_{\text{sd}}}^i)}^{\infty} \frac{\ln(1 + C_1 \varphi_{\mathcal{E}}^* \gamma_{\max}^s \gamma_{r_{\text{sd}}}^s)}{(P_s + P_c) + C_3 \varphi_{\mathcal{E}}^* \gamma_{\max}^s} \exp\left(-\frac{\gamma_{r_{\text{sd}}}^s}{\gamma_{r_{\text{sd}}}^s}\right) \\ & \times \exp\left(-\frac{\gamma_{r_{\text{sd}}}^i}{\gamma_{r_{\text{sd}}}^i}\right) \exp\left(-\frac{\gamma_{\max}^s}{\gamma_{\max}^s}\right) \left(1 - \exp\left(-\frac{\gamma_{\max}^s}{\gamma_{\max}^s}\right)\right)^{L-1} d\gamma_{\max}^s d\gamma_{r_{\text{sd}}}^i d\gamma_{r_{\text{sd}}}^s, \end{aligned} \quad (5.5.16)$$

where $\mathcal{R} = \frac{L}{\gamma_{\max}^s \gamma_{r_{\text{sd}}}^i \gamma_{r_{\text{sd}}}^s}$. The proof of optimal FAEE expression is relegated in Appendix D.10.

Further, we present the expression for upper bound of FAEE for the proposed optimal relaying policy.

Result 29 Upper bound expression for FAEE: *Using the Jensen's inequality to the spectral efficiency term of equation (5.5.9), the upper bound of the FAEE can be expressed as*

$$\begin{aligned} \bar{\mathcal{E}}_{UB} = & \frac{1}{\ln(2)} \ln \left[1 + \mathcal{R} \int_{\gamma_{\max}^s=0}^{\infty} \int_{\gamma_{r_{\text{sd}}}^i=0}^{\infty} \int_{\gamma_{r_{\text{sd}}}^s=\rho'(\gamma_{r_{\text{sd}}}^i)}^{\infty} (C_1 \varphi_{\mathcal{E}}^* \gamma_{\max}^s \gamma_{r_{\text{sd}}}^s) \exp\left(-\frac{\gamma_{r_{\text{sd}}}^s}{\gamma_{r_{\text{sd}}}^s}\right) \right. \\ & \times \exp\left(-\frac{\gamma_{r_{\text{sd}}}^i}{\gamma_{r_{\text{sd}}}^i}\right) \exp\left(-\frac{\gamma_{\max}^s}{\gamma_{\max}^s}\right) \left(1 - \exp\left(-\frac{\gamma_{\max}^s}{\gamma_{\max}^s}\right)\right)^{L-1} d\gamma_{\max}^s d\gamma_{r_{\text{sd}}}^i d\gamma_{r_{\text{sd}}}^s \left. \right] \\ & \times \left[\mathcal{R} \int_{\gamma_{\max}^s=0}^{\infty} \int_{\gamma_{r_{\text{sd}}}^i=0}^{\infty} \int_{\gamma_{r_{\text{sd}}}^s=\rho'(\gamma_{r_{\text{sd}}}^i)}^{\infty} \frac{1}{(P_s + P_c) + C_3 \varphi_{\mathcal{E}}^* \gamma_{\max}^s} \exp\left(-\frac{\gamma_{r_{\text{sd}}}^s}{\gamma_{r_{\text{sd}}}^s}\right) \right. \\ & \times \exp\left(-\frac{\gamma_{r_{\text{sd}}}^i}{\gamma_{r_{\text{sd}}}^i}\right) \exp\left(-\frac{\gamma_{\max}^s}{\gamma_{\max}^s}\right) \left(1 - \exp\left(-\frac{\gamma_{\max}^s}{\gamma_{\max}^s}\right)\right)^{L-1} d\gamma_{\max}^s d\gamma_{r_{\text{sd}}}^i d\gamma_{r_{\text{sd}}}^s \left. \right], \end{aligned} \quad (5.5.17)$$

where $\mathcal{R} = \frac{L}{\gamma_{\max}^s \gamma_{r_{\text{sd}}}^i \gamma_{r_{\text{sd}}}^s}$. The proof of optimal FAEE expression is relegated in Appendix D.11.

Remarks: The analytical expression obtained for FAEE and its upper bound is a triple integral expression. Further simplification can be performed numerically. Note that both these equations cannot be simplified into a closed-form expression because of the presence of $\varphi_{\mathcal{E}}^*$. Since the solution of the $\varphi_{\mathcal{E}}^*$ is obtained through the transcendental equation.

5.6 Numerical Results and Benchmarking for EH C-SSS

In this section, we evaluate the proposed IC-PA-DAF relay-assisted underlay C-SSS performance with EHRS adopted to select the best relay. To analyze the validity of the analytical results derived, we use monte-carlo simulations. Further, to study the performance improvement of the proposed policy, we compare it with benchmark policies. For the comparison purpose, we have used two benchmark policies, 1.) Simple DAF relay-assisted underlay C-SSS with EHRS policy, and 2.) Simple DAF relay-assisted underlay C-SSS with RRS policy. It is essential to mention that for a fair comparison, we have considered that the transmit power of the selected relay is interference-constrained to avoid interference in the system model with benchmark policies. In Table 5.2, we present the simulation parameters used to generate simulation plots.

Table 5.2: Simulation parameters for EH relay-assisted underlay C-SSS model.

Simulation Parameter	Value	Symbol
Number of channel realizations	10^5	N
Number of relays	2	L
Time Slot	1 s	T
Energy harvesting duty cycle	0.4	τ
Energy conversion efficiency	80%	η
Power consumed by the circuitry	15 dBm	P_c
Source node to relay node distance in secondary cloud	1 m	d_s
Relay node to destination node distance in secondary cloud	1 m	D_s
Path loss exponent	2.7	ν
Symbol energy	1	$ \alpha ^2$

Below we present the simulation plots for analyzing the performance of the proposed system model.

Analysis of FASE vs source transmit power: Figure 5.7 plots FASE with respect to the source transmit power. In this plot, the initial observations are that as the source transmit power increases, the FASE for benchmark policies increases because the energy harvested by the relays increases. However, we observe that the FASE plot

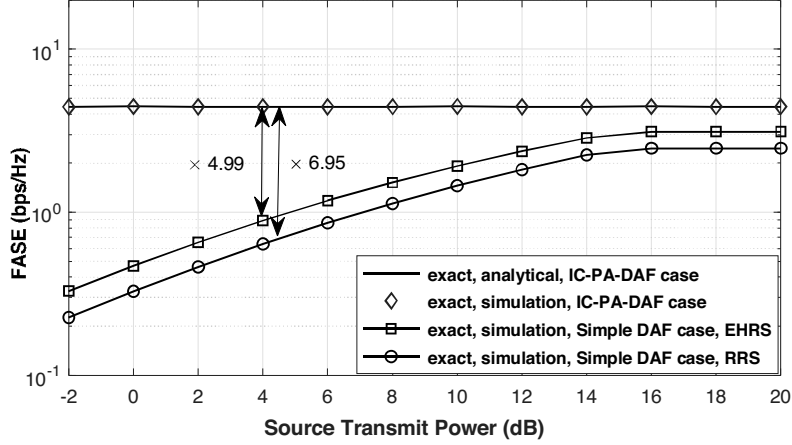


Figure 5.7: FASE as a function of source transmit power ($\tau = 0.4$, $d_s = 1$ m, $\eta = 0.8$, average channel power gain of all links = 1, $D_s = 1$ m, $L = 2$, and $\sigma_d = 1$).

of the proposed policy remains constant because of the typical nature of the proposed IC-PA-DAF relay which amplifies the forwarding signal adaptively and keeps the proposed policy's performance excellent for low and medium SNR ranges as well. Further, we can observe that the performance of the proposed policy outperforms the benchmark policies. Typically, we observe a performance improvement of 5 times with respect to simple DAF case with EHRS and performance improvement of 7 times in comparison to simple DAF case with RRS at 4 dB.

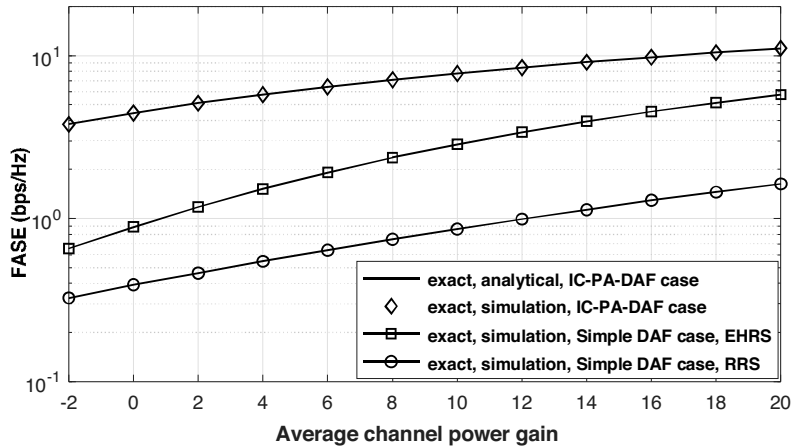


Figure 5.8: FASE as a function of average channel power gain of $R_S^s - D_{R_x}^s$ link ($\tau = 0.4$, $d_s = 1$ m, $\eta = 0.8$, $P_s = 4$ dB, $D_s = 1$ m, $L = 2$, and $\sigma_d = 1$).

Analysis of FASE vs average channel power gain of $R_S^s - D_{R_x}^s$ link: Figure 5.8 plots FASE as a function of average channel power gain of $R_S^s - D_{R_x}^s$ link. In this plot, the initial observation is that as the mean channel power gain of the $R_S^s - D_{R_x}^s$ link increases, the FASE increases because of the increase in the SNR at the destination. Further, we also observe that the proposed policy performs better than the benchmark

policies, and the upper bound of the proposed policy tracks the exact plot well.

Impact of I_{th} on FASE: Figure 5.9 plots FASE as a function of source transmit

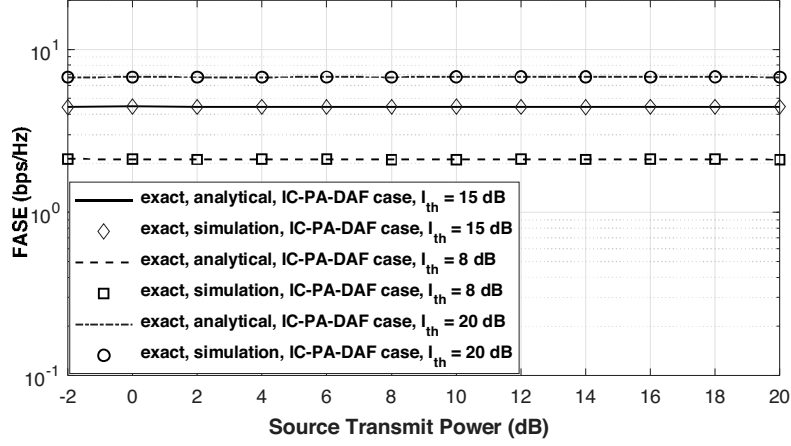


Figure 5.9: FASE as a function of source transmit power for various I_{th} value ($\tau = 0.4$, $d_s = 1$ m, $\eta = 0.8$, average channel power gain of all links = 1, $D_s = 1$ m, $L = 2$, and $\sigma_d = 1$).

power for various I_{th} values. In the plot we observe that due to IC-PA-DAF relaying policy, the performance of the system model in terms of FASE is better. Further, we analyze that as the value of I_{th} increases, the FASE of the system model also increases.

Impact of source transmit power on FAEE: Figure 5.10 plots FAEE as a function

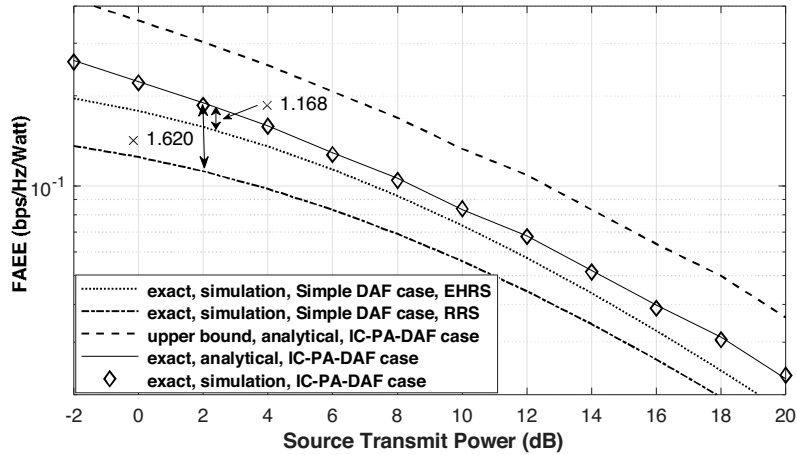


Figure 5.10: FAEE as a function of source transmit power ($\tau = 0.4$, $d_s = 1$ m, $\eta = 0.8$, average channel power gain of all links = 1, $D_s = 1$ m, $L = 2$, $P_c = 15$ dBm, and $\sigma_d = 1$).

of source transmit power. In this plot, we observe that as the source transmit power increases, the energy efficiency decreases. This happens as the overall utilization of the energy resources has increased. Further, the proposed policy is validated through

monte-carlo simulation, and its upper bound tracks the exact plot well. Lastly, the proposed policy outperforms the benchmark policy. Typically, a performance improvement of 1.16 times and 1.6 times is achieved in comparison to single DAF case with EHRS and simple DAF case with RRS, respectively at 4 dB.

Impact of average channel power gain of $R_S^s - D_{Rx}^s$ link on FAEE: Figure 5.11

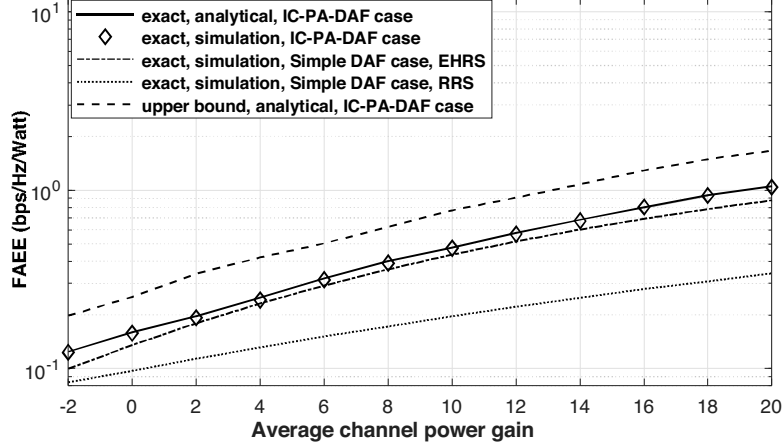


Figure 5.11: FAEE as a function of average channel power gain of $R_S^s - D_{Rx}^s$ link ($\tau = 0.4$, $d_s = 1$ m, $\eta = 0.8$, average channel power gain of all links = 1, $D_s = 1$ m, $L = 2$, $P_s = 4$ dB, $P_c = 15$ dBm and $\sigma_d = 1$).

plots FAEE as a function of the average channel power gain of the $R_S^s - D_{Rx}^s$ link. In this plot, we observe that as the mean channel power gain increases, the FAEE also increases. This happens due to the increase in the SNR at the secondary destination. Further, the proposed policy performs better in comparison to the benchmark policies.

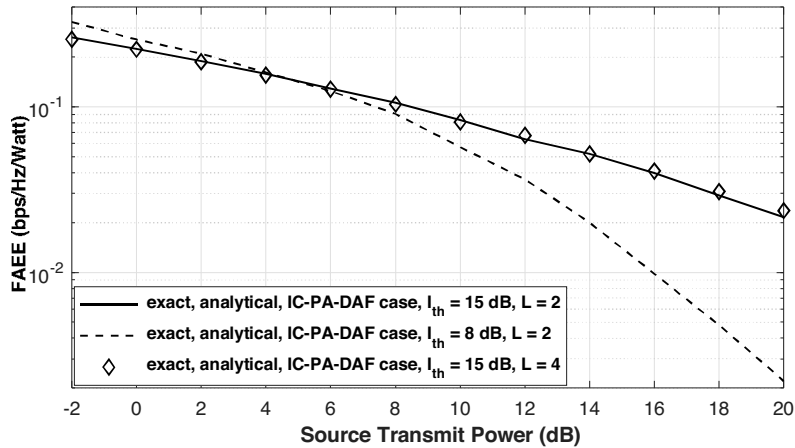


Figure 5.12: FAEE as a function of source transmit power for various L and I_{th} values ($\tau = 0.4$, $d_s = 1$ m, $\eta = 0.8$, average channel power gain of all links = 1, $D_s = 1$ m, $L = 2$, and $\sigma_d = 1$).

Impact of I_{th} and L on FAEE: Figure 5.12 shows the FAEE versus source transmit

power plot for different values of L and I_{th} . The figure shows that the variation in the number of relays does not change the FAEE performance measure for the proposed IC-PA-DAF relaying policy. However, this does not stand true when the value of I_{th} is varied. It can be observed that high energy efficiency can be achieved for high I_{th} value in the medium and high SNR regime.

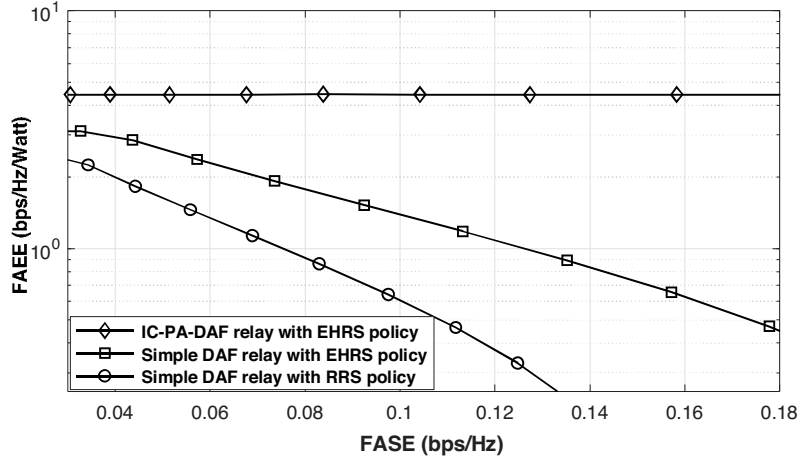


Figure 5.13: FAEE versus FASE trade-off ($\tau = 0.4$, $d_s = 1$ m, $\eta = 0.8$, average channel power gain of all links = 1, $D_s = 1$ m, $P_c = 15$ dBm, $L = 2$, and $\sigma_d = 1$).

FAEE vs. FASE trade-off: Figure 5.13 plots the trade-off between the FAEE and FASE. From the plot, it can be observed that for the proposed policy, the FAEE remains high and almost constant for varying FASE. Hence a negligible trade-off can be observed for the proposed policy. However, for both the benchmark policies, FAEE decreases with the increase in FASE, which shows the trade-off between FAEE and FASE for the benchmark policies.

5.7 Summary

Initially in this chapter, we considered a two-hop, and two IC-PA-DAF relay-assisted C-SSS model. For it, we formulated new optimization problems and derived their solutions. The proposed optimal relaying policy sets the IC-PA-DAF relay's transmit power to meet the average interference constraint. We evaluated the proposed relaying policy's performance in terms of FASE and FAEE. To see the performance improvement, we compared the proposed policy with benchmark policies. We found that the proposed policy outperforms the benchmark relaying policies, enabling the use of IC-PA-DAF policy. Specifically, we see that the proposed policy achieves energy efficiency 1.7 times higher compared to the fixed gain DAF policy for the non-EH system model.

Further, in this chapter, we considered a more generalized system model with multiple relays having EH capabilities. For this model, we proposed a IC-PA-DAF relaying policy. In it, the relay selected (based on EHRS policy) performs decoding, re-encoding and adaptive amplification based on the RGF. For the proposed system model, we presents optimization problem to enhance two very critical performance measures, that are, FASE and FAEE. Based on the optimization problem, we further derive optimum RGF and use it to derive FASE and FAEE. We presented a comprehensive and analytically rich performance analysis for the optimal policies. Specifically, we derived the analytical expressions for the performance measures. Furthermore, we presented extensive numerical results to validate the derived analytical expressions and showed that the proposed optimal relaying policies outperform the benchmark policies. Quantitatively, we observed that the proposed policy achieves energy efficiency performance gain of 1.2 times higher compared to the simple DAF policy for the EH relay-assisted system model.